2202 *Inorg. Chem.* **2010**, *49*, 2202–2209
DOI: 10.1021/ic902024s

Inorganic Chemistry
Article

Insight into Water Oxidation by Mononuclear Polypyridyl Ru Catalysts

Derek J. Wasylenko,[†] Chelladurai Ganesamoorthy,[†] Bryan D. Koivisto,[†] Matthew A. Henderson,[‡] and Curtis P. Berlinguette*[,†]

[†]*Department of Chemistry and Institute for Sustainable Energy, Environment & Economy, University of Calgary, 2500 University Drive N.W., Calgary T2N-1N4, Canada, and* [‡]*Department of Chemistry, University of Victoria, Victoria, British Columbia V38-3 V6, Canada*

Received October 13, 2009

A family of compounds based on the mononuclear coordination complex $[Ru(tpy)(bpy)(OH_2)]^{2+}$ (**1b**; tpy=2,2′:6′,2″-terpyridine, bpy=2,2′-bipyridine) are shown to be competent catalysts in the Ce(IV)-driven oxidation of water in acidic media. The systematic installation of electron-withdrawing (e.g., −Cl, −COOH) and −donating (e.g., −OMe) groups at various positions about the periphery of the polypyridyl framework offers insight into how electronic parameters affect the properties of water oxidation catalysts. It is observed, in general, that electron-withdrawing groups (EWGs) on the bpy ligands suppress catalytic activity (k_{obs}) and enhance catalytic turnover numbers (TONs); conversely, the presence of electron-donating groups (EDGs) accelerate catalytic rates while decreasing catalyst stability. We found that 2,2′-bipyridine *N,N′*-dioxide is produced when **1b** is subject to excess Ce(IV) in acidic media, which suggests that dissociation of the bpy ligand is a source of catalyst deactivation and/or decomposition. Density functional theory (DFT) calculations corroborate these findings by showing that the $Ru-N_{bpy}$ bond *trans* to the O atom is weakened at higher oxidation levels while the other Ru−N bonds are affected to a lesser extent. We also show that the Ru−Cl bond is not robust in aqueous media, which has implications in studying the catalytic behavior of systems of this type.

Introduction

Homogenous water oxidation catalysts typically feature the following design elements: (i) a suitable redox-active metal center; (ii) an oxidatively stable coordination environment; and (iii) a coordination site occupied by a labile ligand (e.g., solvent, halide).[1−9] While it was long thought that multiple metal centers are required to carry out the multiple proton-coupled electron-transfer (PCET) steps[10] associated with water splitting,[11] it has recently been shown that mononuclear complexes are capable of mediating the formation of dioxygen from water. This feature was first established by Bernhard et al.[12] for a suite of Ir complexes, while Thummel et al.,[13] Meyer et al.,[14] and Sakai et al.[15] followed up with independent findings that polypyridyl Ru compounds are also competent catalysts. This observation has important implications in the study of homogeneous water oxidation catalysts because mononuclear systems are generally easier to synthesize and study than systems of higher nuclearity.[16,17] This statement is corroborated by a relatively well-defined catalytic mechanism of water oxidation by mononuclear polypyridyl Ru complexes.[18]

*To whom correspondence should be addressed. E-mail: cberling@ucalgary.ca.

(1) Yagi, M.; Kaneko, M. *Chem. Rev.* **2001**, *101*, 21–35.
(2) Sala, X.; Romero, I.; Rodriguez, M.; Escriche, L.; Llobet, A. *Angew. Chem., Int. Ed.* **2009**, *48*, 2842–2852.
(3) Liu, F.; Concepcion, J. J.; Jurss, J. W.; Cardolaccia, T.; Templeton, J. L.; Meyer, T. J. *Inorg. Chem.* **2008**, *47*, 1727–1752.
(4) Romero, I.; Rodriguez, M.; Sens, C.; Mola, J.; Kollipara, M. R.; Francas, L.; Mas-Marza, E.; Escriche, L.; Llobet, A. *Inorg. Chem.* **2008**, *47*, 1824–1834.
(5) Betley, T. A.; Wu, Q.; Van Voorhis, T.; Nocera, D. G. *Inorg. Chem.* **2008**, *47*, 1849–1861.
(6) Limburg, J.; Vrettos, J. S.; Liable-Sands, L. M.; Rheingold, A. L.; Crabtree, R. H.; Brudvig, G. W. *Science* **1999**, *283*, 1524–1527.
(7) Geletii, Y. V.; Botar, B.; Köegerler, P.; Hillesheim, D. A.; Musaev, D. G.; Hill, D. L. *Angew. Chem., Int. Ed.* **2008**, *47*, 3896–3899.
(8) Sartorel, A.; Carraro, M.; Scorrano, G.; De Zorzi, R.; Geremia, S.; McDaniel, N. D.; Bernhard, S.; Bonchio, M. *J. Am. Chem. Soc.* **2008**, *130*, 5006–5007.
(9) Wada, T.; Tsuge, K.; Tanaka, K. *Inorg. Chem.* **2001**, *40*, 329–337.
(10) Huynh, M. H. V.; Meyer, T. J. *Chem. Rev.* **2007**, *107*, 5004–5064.
(11) Eisenberg, R.; Gray, H. B. *Inorg. Chem.* **2008**, *47*, 1697–1699.
(12) McDaniel, N. D.; Coughlin, F. J.; Tinker, L. L.; Bernhard, S. *J. Am. Chem. Soc.* **2008**, *130*, 210–217.
(13) Tseng, H.; Zong, R.; Muckerman, J. T.; Thummel, R. *Inorg. Chem.* **2008**, *47*, 11763–11773.
(14) Concepcion, J. J.; Jurss, J. W.; Templeton, J. L.; Meyer, T. J. *J. Am. Chem. Soc.* **2008**, *130*, 16462–16463.
(15) Masaoka, S.; Sakai, K. *Chem. Lett.* **2009**, *38*, 182–183.
(16) Concepcion, J. J.; Jurss, J. W.; Norris, M. R.; Chen, Z.; Templeton, J. L.; Meyer, T. J. *Inorg. Chem.*, **2010**, ASAP; DOI: 10.1021/ic901437e.
(17) Duan, L.; Xu, Y.; Zhang, P.; Wang, M.; Sun, L. *Inorg. Chem.* **2010**, *49*, 209–215.
(18) Concepcion, J. J.; Jurss, J. W.; Brennaman, M. K.; Hoertz, P. G.; Patrocinio, A. O. T.; Murakami Iha, N. Y.; Templeton, J. L.; Meyer, T. J. *Acc. Chem. Res.* **2009**, *42*, 1954–1965.

Published on Web 02/04/2010

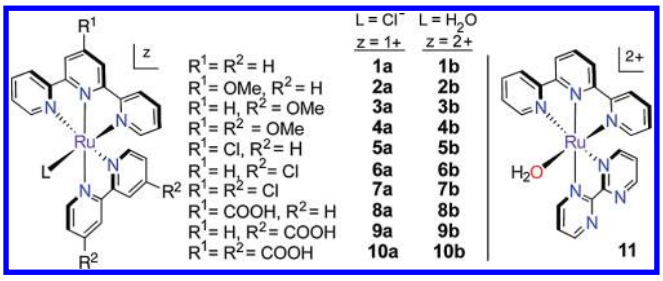

Figure 1. Mononuclear Ru complexes investigated in this study. (Counterion = Cl^- for **1a**−**10a**; ClO_4^- for **1b**−**10b** and **11**.[14]).

Taking into account that there remain a number of questions surrounding water oxidation by mononuclear and higher order catalysts,[11,19−21] we set out to examine the coordination complex $[Ru(tpy)(bpy)(OH_2)]^{2+}$ (**1b**; tpy = 2,2′:6′,2″-terpyridine, bpy = 2,2′-bipyridine; Figure 1) in the context of water oxidation.[15] By installing electron-donating and withdrawing substituents about the periphery of the polypyridyl ligands (i.e., **2b**−**10b**; Figure 1), we are able to extrapolate how electronic parameters affect catalyst activity and stability while holding the local ligand environment at parity. This strategy provides specific insight into how electronic parameters affect the activity and stability of mononuclear polypyridyl Ru catalysts related to **1b**. A summary of these results is reported herein, as well as an evaluation of other issues critical to assessing Ru-catalyzed water oxidation.

Experimental Section

Preparation of Compounds. All reactions and manipulations were performed using solvents passed through an MBraun solvent purification system prior to use. Unless stated otherwise, all reagents were purchased from Aldrich and used without further purification; 4,4′-dichloro-2,2′-bipyridine (bpy-Cl) was purchased from BOC Sciences; 2,2′-bipyridine-4,4′-dicarboxylic (bpy-COOH) acid was purchased from Alfa Aesar, and $RuCl_3 \cdot 3H_2O$ was purchased from Pressure Chemical Company. Purification by column chromatography was carried out using silica (Silicycle: Ultrapure Flash Silica). Analytical thin-layer chromatography (TLC) was performed on aluminum-backed sheets precoated with silica 60 F254 adsorbent (0.25 mm thick; Merck, Germany). ^{1}H NMR chemical shifts (δ) are reported in parts per million (ppm) from low to high field and referenced to residual non-deuterated solvent. Standard abbreviations indicating multiplicity are used as follows: br = broad; s = singlet; d = doublet; t = triplet; m = multiplet. All proton assignments correspond to the generic molecular scheme depicted in Figure 2. Ligands 4′-methoxy-2,2′:6′,2″-terpyridine (tpy-OMe),[22] 4′-chloro-2,2′:6′,2″-terpyridine (tpy-Cl),[23] and 2,2′:6′,2″-terpyridine-4′-carboxylic acid (tpy-COOH)[24] were prepared according to published procedures. Complexes $Ru(tpy)Cl_3$ (**I**),[25] and $[Ru(tpy)(bpm)(OH_2)](ClO_4)_2$ (**11b**)[14] were prepared using the synthetic and purification steps detailed below.

General Synthetic Procedure for Ru(tpy-R^1)Cl$_3$ (I−IV). $RuCl_3 \cdot 3H_2O$ (0.70 mmol) and tpy-R^1 (0.70 mmol) were combined in 50 mL of EtOH and refluxed for 4 h. The mixture was cooled, and the product was collected as a red/purple solid upon filtration.

Ru(tpy-OMe)Cl$_3$ (II). Yield: 83%; ESI-MS: m/z (%): 435 $[(M-Cl)^+]$ (anal. calcd for $C_{16}H_{13}Cl_2N_3ORu^+$: $m/z = 434.95$).

Ru(tpy-Cl)Cl$_3$ (III). Yield: 85%; ESI-MS: m/z: 441 $[(M-Cl)^+]$ (anal. calcd for $C_{15}H_{10}Cl_3N_3Ru^+$: $m/z = 440.90$).

Ru(tpy-COOH)Cl$_3$ (IV). Yield: 89%; ESI-MS: m/z: 449 $[(M-Cl)^+]$ (anal. calcd for $C_{16}H_{11}Cl_2N_3O_2Ru^+$: $m/z = 448.93$).

General Synthetic Procedure for [Ru(tpy-R^1)(bpy-R^2)Cl]Cl (1a−10a). Ru(tpy-R^1)Cl$_3$ (0.70 mmol) and bpy-R^2 (0.70 mmol) were combined with LiCl (7.0 mmol) and *N*-ethylmorpholine (0.5 mL) in 30 mL of MeOH/H_2O (5:1). The mixture was then heated at reflux for 3 h. The solvent was removed from the solution, and the crude product dry-loaded onto silica. The product was collected as a deep purple-colored band using acetone/methanol/water (3:1:1) saturated with LiCl as the eluent. Typical R_f values for the purple band were 0.65−0.75. The product fractions were combined, and the solvent removed to near dryness (∼15 mL), and then 1 mL of concentrated HCl was added to precipitate the product. The purple solid was then washed with 10 mL of 1 M HCl and left to air-dry. Yields and characterization are given below.

[Ru(tpy)(bpy)Cl]Cl (1a). Yield: 75%; ^{1}H NMR (400 MHz, [D$_6$]DMSO): $\delta = 10.10$ (d, ^3J(H,H) = 5.0 Hz, 1H; H_A), 8.93 (d, ^3J(H,H) = 8.2 Hz, 1H; H_D), 8.83 (d, ^3J(H,H) = 8.1 Hz, 2H; H_e), 8.71 (d, ^3J(H,H) = 8.1 Hz, 2H; H_d), 8.64 (d, ^3J(H,H) = 8.2 Hz, 1H; H_E), 8.35 (ddd, ^3J(H,H) = 8.0, 7.9 Hz, ^4J(H,H) = 1.5 Hz, 1H; H_C), 8.21 (t, ^3J(H,H) = 8.1 Hz, 1H; H_f), 8.07 (ddd, ^3J(H,H) = 7.0, 5.7 Hz, ^4J(H,H) = 1.0 Hz, 1H; H_B), 7.98 (ddd, ^3J(H,H) = 8.0, 7.9 Hz, ^4J(H,H) = 1.5 Hz, 2H; H_c), 7.78 (ddd, ^3J(H,H) = 8.0, 7.9 Hz, ^4J(H,H) = 1.4 Hz, 1H; H_F), 7.62 (d, ^3J(H,H) = 5.5 Hz, 2H; H_a), 7.38 (ddd, ^3J(H,H) = 7.5, 5.5 Hz, ^4J(H,H) = 1.2 Hz, 2H; H_b), 7.32 (d, ^3J(H,H) = 5.6 Hz, 1H; H_H), 7.09 (ddd, ^3J(H,H) = 7.3, 5.7 Hz, ^4J(H,H) = 1.3 Hz, 1H; H_G). λ_{max} (MeCN) (ε (M^{-1} cm^{-1}): 503 nm (9.5×10^3). ESI-MS: m/z: 526 $[(M-Cl)^+]$ (anal. calcd for $C_{25}H_{19}ClN_5ORu^+$: m/z = 526.04); elemental analysis calcd (%) for $C_{25}H_{19}Cl_2N_5Ru \cdot 3H_2O$: C 48.79, H 4.09, N 11.38; found: C 48.87, H 4.33, N 11.51.

[Ru(tpy-OMe)(bpy)Cl]Cl (2a). Yield: 76%; ^{1}H NMR (400 MHz, CD_3CN): $\delta = 10.20$ (d, ^3J(H,H) = 4.0 Hz, 1H; H_A), 8.58 (d, ^3J(H,H) = 8.0 Hz, 1H; H_D), 8.40 (d, ^3J(H,H) = 8.0 Hz, 2H; H_d), 8.31 (d, ^3J(H,H) = 8.0 Hz, 1H; H_E), 8.21 (ddd, ^3J(H,H) = 7.6 Hz, ^4J(H,H) = 1.2 Hz, 1H; H_C), 8.14 (s, 2H; H_e), 7.91 (ddd, ^3J(H,H) = 6.4 Hz, ^4J(H,H) = 1.2 Hz, 1H; H_B), 7.86 (ddd, 2H, ^3J(H,H) = 8.0 Hz, ^4J(H,H) = 1.6 Hz; H_c), 7.66 (m, 3H; $H_{a,F}$), 7.39 (d, ^3J(H,H) = 5.2 Hz, 1H; H_H), 7.24 (ddd, ^3J(H,H) = 7.6 Hz, ^4J(H,H) = 1.2 Hz, 2H; H_b), 6.96 (ddd, ^3J(H,H) = 7.6 Hz, ^4J(H,H) = 1.6 Hz, 1H; H_G), 4.21 (s, 3H; OMe). λ_{max} (MeCN) (ε (M^{-1} cm^{-1}): 508 nm (10.6×10^3). ESI-MS: m/z: 556 $[(M-Cl)^+]$ (anal. calcd for $C_{26}H_{21}ClN_5ORu^+$: m/z = 556.05); elemental analysis calcd (%) for $C_{26}H_{21}Cl_2N_5ORu \cdot 4H_2O$: C 47.06, H 4.41, N 10.55; found: C 47.25, H 4.33, N 10.61.

[Ru(tpy)(bpy-OMe)Cl]Cl (3a). Yield: 52%; ^{1}H NMR (400 MHz, [D$_6$]DMSO): $\delta = 9.83$ (d, ^3J(H,H) = 6.8 Hz, 1H; H_A), 8.79 (d, ^3J(H,H) = 8.0 Hz, 2H; H_e), 8.67 (d, ^3J(H,H) = 8.0 Hz 2H; H_d), 8.58 (d, ^4J(H,H) = 2.4 Hz, 1H; H_D), 8.31 (d, ^4J(H,H) = 2.4 Hz, 1H; H_E), 8.14 (t, ^3J(H,H) = 8.0 Hz, 1H; H_f), 7.96 (t, ^3J(H,H) = 7.6 Hz, 2H; H_c), 7.74 (dd, ^3J(H,H) = 7.2 Hz, ^4J(H,H) = 2.4 Hz, 1H; H_B), 7.71 (d, ^3J(H,H) = 5.2 Hz, 2H; H_a), 7.40 (t, ^3J(H,H) = 6.4 Hz, 2H; H_b), 7.93 (d, ^3J(H,H) = 6.8 Hz, 1H; H_H), 6.70 (dd, ^3J(H,

(19) Hurst, J. K.; Cape, J. L.; Clark, A. E.; Das, S.; Qin, C. *Inorg. Chem.* **2008**, *47*, 1753–1764.
(20) Binstead, R. A.; Chronister, C. W.; Ni, J.; Hartshorn, C. M.; Meyer, T. J. *J. Am. Chem. Soc.* **2000**, *122*, 8464–8473.
(21) Bozoglian, F.; Romain, S.; Ertem, M. Z.; Todorova, T. K.; Sens, C.; Mola, J.; Rodriguez, M.; Romero, I.; Benet-Buchholz, J.; Fontrodona, X.; Cramer, C. J.; Gagliardi, L.; Llobet, A. *J. Am. Chem. Soc.* **2009**, *131*, 15176–15187.
(22) Chambers, J.; Eaves, B.; Parker, D.; Claxton, R.; Ray, P. S.; Slattery, S. J. *Inorg. Chim. Acta* **2006**, *359*, 2400–2406.
(23) Constable, E. C.; Ward, M. D. *J. Chem. Soc., Dalton Trans.* **1990**, 1405–1409.
(24) Wolpher, H.; Sinha, S.; Pan, J. X.; Johansson, A.; Lundqvist, M. J.; Persson, P.; Lomoth, R.; Bergquist, J.; Sun, L. C.; Sundstrom, V.; Akermark, B.; Polivka, T. *Inorg. Chem.* **2007**, *46*, 638–651.
(25) Winter, A.; Hummel, J.; Risch, N. *J. Org. Chem.* **2006**, *71*, 4862–4871.

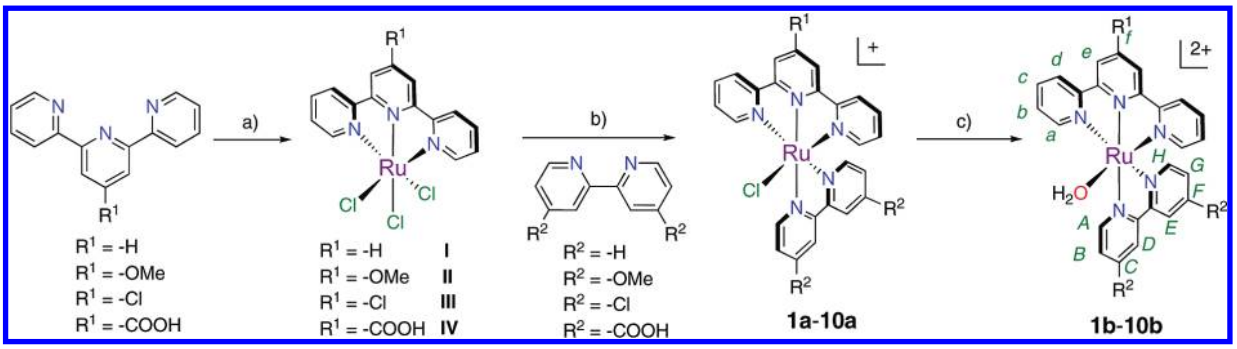

Figure 2. General synthetic procedure for the **1a**−**10a** and **1b**−**10b**: (a) $RuCl_3 \cdot 3H_2O$, EtOH, reflux, 3 h; (b) 10 equiv LiCl, *N*-ethylmorpholine, MeOH:H_2O (5:1), reflux, 3 h; (c) 2 equiv $AgClO_4$, H_2O, reflux, 3 h. The ^1H NMR labeling scheme is provided for **1b**−**10b**; the labeling is analogous for **1a**−**10a**.

H) = 6.8 Hz, ^4J(H,H) = 2.8 Hz, 1H; H_G), 4.18 (s, 3H; OMe), 3.82 (s, 3H; OMe). λ_{max} (MeCN) (e (M^{-1} cm^{-1}): 513 nm (10.7 × 10^3). ESI-MS: *m*/*z*: 586 [(M−Cl)$^+$] (anal. calcd for $C_{27}H_{23}ClN_5O_2Ru^+$: *m*/*z* = 586.06); elemental analysis calcd (%) for $C_{27}H_{23}Cl_2N_5O_2Ru \cdot 4H_2O \cdot LiCl$: C 44.06, H 4.25, N 9.52; found: C 44.27, H 4.28, N 9.48.

[Ru(tpy-OMe)(bpy-OMe)Cl]Cl (4a). Yield: 74%; ^1H NMR (400 MHz, CD_3CN): δ = 9.91 (d, ^3J(H,H) = 6.8 Hz, 1H; H_A), 8.38 (d, ^3J(H,H) = 8.0 Hz, 2H; H_d), 8.13 (d, ^4J(H,H) = 2.8 Hz, 1H; H_D), 8.11 (s, 2H; H_e), 7.85 (m, 3H; $H_{E,c}$), 7.75 (d, ^3J(H,H) = 5.6 Hz, 2H; H_a), 7.51 (dd, ^3J(H,H) = 6.4 Hz, ^4J(H,H) = 2.8 Hz, 2H; H_B), 7.26 (ddd, ^3J(H,H) = 7.6 Hz, ^4J(H,H) = 1.2 Hz, 2H; H_b), 7.06 (d, ^3J(H,H) = 6.8 Hz, 1H; H_H), 6.54 (dd, ^3J(H,H) = 6.4 Hz, ^4J(H,H) = 2.8 Hz, 1H; H_G), 4.20 (s, 3H; OMe), 4.16 (s, 3H; OMe), 3.83 (s, 3H; OMe). λ_{max} (MeCN) (ε (M^{-1} cm^{-1}): 517 nm (11.6 × 10^3). ESI-MS: *m*/*z*: 616 [(M−Cl)$^+$] (anal. calcd for $C_{28}H_{25}ClN_5O_3Ru^+$: *m*/*z* = 616.06); elemental analysis calcd (%) for $C_{28}H_{25}Cl_2N_5O_3Ru \cdot H_2O$: C 50.23, H 4.06, N 10.46; found: C 49.89, H 4.09, N 10.36.

[Ru(tpy-Cl)(bpy)Cl]Cl (5a). Yield: 63%; ^1H NMR (400 MHz, [D_6]DMSO): δ = 10.07 (d, ^3J(H,H) = 4.8 Hz, 1H; H_A), 9.09 (s, 2H; H_e), 8.95 (d, ^3J(H,H) = 8.1 Hz, 1H; H_D), 8.80 (d, ^3J(H,H) = 8.0 Hz, 2H; H_d), 8.66 (d, ^3J(H,H) = 8.0 Hz, 1H; H_E), 8.37 (ddd, ^3J(H,H) = 7.8, 7.7 Hz, ^4J(H,H) = 1.4 Hz, 1H; H_C), 8.07 (ddd, ^3J(H,H) = 7.2, 7.0 Hz, ^4J(H,H) = 1.0 Hz, 1H; H_B), 8.01 (ddd, ^3J(H,H) = 7.8, 7.7 Hz, ^4J(H,H) = 1.3 Hz, 2H, H_c), 7.78 (ddd, ^3J(H,H) = 8.1, 8.0 Hz, ^4J(H,H) = 1.2 Hz, 1H; H_F), 7.64 (d, ^3J(H,H) = 4.9 Hz, 2H; H_a), 7.44 (d, ^3J(H,H) = 5.3 Hz, 1H; H_H), 7.41 (ddd, ^3J(H,H) = 8.1, 8.0 Hz, ^4J(H,H) = 1.1 Hz, 2H; H_b), 7.06 (ddd, ^3J(H,H) = 7.2, 7.0 Hz, ^4J(H,H) = 1.0 Hz, 1H; H_G). λ_{max} (MeCN) (ε (M^{-1} cm^{-1}): 507 nm (9.8 × 10^3). ESI-MS: *m*/*z*: 560 [(M−Cl)$^+$] (anal. calcd for $C_{25}H_{18}Cl_2N_5Ru^+$: *m*/*z* = 560.00); elemental analaysis calcd (%) for $C_{25}H_{18}Cl_3N_5Ru \cdot 4H_2O$: C 44.95, H 3.92, N 10.49; found: C 45.02, H 3.96, N 10.40.

[Ru(tpy)(bpy-Cl)Cl]Cl (6a). Yield: 54%; ^1H NMR (400 MHz, [D_6]DMSO): δ = 10.00 (d, ^3J(H,H) = 6.0 Hz, 1H; H_A), 9.24 (d, ^4J(H,H) = 2.4 Hz, 1H; H_D), 8.98 (d, ^4J(H,H) = 2.0 Hz, 1H; H_E), 8.82 (d, ^3J(H,H) = 8.0 Hz, 2H; H_e), 8.69 (d, ^3J(H,H) = 8.0 Hz, 2H; H_d), 8.23 (m, 2H; $H_{B,f}$), 8.00 (ddd, ^3J(H,H) = 7.6 Hz, ^4J(H,H) = 1.2 Hz, 2H; H_c), 7.71 (d, ^3J(H,H) = 4.8 Hz, 2H; H_a), 7.38 (ddd, ^3J(H,H) = 5.6 Hz, ^4J(H,H) = 1.2 Hz, 2H; H_b), 7.33 (d, ^3J(H,H) = 6.0 Hz, 1H; H_G), 7.21 (ddd, ^3J(H,H) = 6.0 Hz, ^4J(H,H) = 2.4 Hz, 1H; H_H). λ_{max} (MeCN) (ε (M^{-1} cm^{-1}): 519 nm (11.9 × 10^3). ESI-MS: *m*/*z*: 596 [(M−Cl)$^+$] (anal. calcd for $C_{25}H_{17}Cl_3N_5Ru^+$: *m*/*z* = 595.96); elemental analysis calcd (%) for $C_{25}H_{17}Cl_4N_5Ru \cdot 3H_2O$: C 43.88, H 3.39, N 10.23; found: C 43.88, H 3.29, N 10.04.

[Ru(tpy-Cl)(bpy-Cl)Cl]Cl (7a). Yield: 60%; ^1H NMR (400 MHz, [D_6]DMSO): δ = 9.97 (d, ^3J(H,H) = 6.4 Hz, 1H; H_A), 9.24 (d, ^4J(H,H) = 2.0 Hz, 1H; H_D), 9.08 (s, 2H; H_e), 8.98 (d, ^4J(H,H) = 2.4 Hz, 1H; H_E), 8.77 (d, ^3J(H,H) = 8.0 Hz, 2H; H_d), 8.23 (dd, ^3J(H,H) = 6.0 Hz, ^4J(H,H) = 1.6 Hz, 1H; H_B), 8.02 (t, ^3J(H,H) = 8.0 Hz, 2H; H_c), 7.74 (d, ^3J(H,H) = 5.2 Hz, 2H; H_a), 7.47 (d, ^3J(H,H) = 6.4 Hz, 1H; H_G), 7.40 (t, ^3J(H,H) = 6.8 Hz, 2H; H_b), 7.18 (dd, ^3J(H,H) = 6.4 Hz, ^4J(H,H) = 2.0 Hz, 1H; H_H). λ_{max} (MeCN) (ε (M^{-1} cm^{-1}): 520 nm (13.2 × 10^3). ESI-MS: *m*/*z*: 630 [(M−Cl)$^+$] (anal. calcd for $C_{25}H_{16}Cl_4N_5Ru^+$: *m*/*z* = 629.92); elemental analysis calcd (%) for $C_{25}H_{16}Cl_5N_5Ru \cdot 2H_2O$: C 42.85, H 2.88, N 9.99; found: C 42.81, H 2.61, N 9.87.

[Ru(tpy-COOH)(bpy)Cl]Cl (8a). Yield: 61%; ^1H NMR (400 MHz, [D_6]DMSO): δ = 10.10 (d, ^3J(H,H) = 4.0 Hz, 1H; H_A), 9.14 (s, 2H; H_e), 8.95 (d, ^3J(H,H) = 8.0 Hz, 1H; H_D), 8.90 (d, ^3J(H,H) = 8.0 Hz, 2H; H_d), 8.66 (d, ^3J(H,H) = 8.0 Hz, 1H; H_E), 8.40 (ddd, ^3J(H,H) = 8.0 Hz, ^4J(H,H) = 1.6 Hz, 1H; H_C), 8.10 (ddd, ^3J(H,H) = 6.8 Hz, ^4J(H,H) = 1.2 Hz, 1H; H_B), 7.99 (ddd, ^3J(H,H) = 8.0 Hz, ^4J(H,H) = 1.6 Hz, 2H; H_c), 7.79 (ddd, ^3J(H,H) = 8.0 Hz, ^4J(H,H) = 1.2 Hz, 1H; H_F), 7.64 (d, ^3J(H,H) = 5.6 Hz, 1H; H_a), 7.42 (ddd, ^3J(H,H) = 5.6 Hz, ^4J(H,H) = 1.2 Hz, 2H; H_b), 7.33 (d, ^3J(H,H) = 5.2 Hz, 1H; H_H), 7.04 (ddd, ^3J(H,H) = 6.0 Hz, ^4J(H,H) = 1.2 Hz, 1H; H_G). λ_{max} (MeOH) (ε (M^{-1} cm^{-1}): 505 nm (11.0 × 10^3). ESI-MS: *m*/*z*: 570 [(M−Cl)$^+$] (anal. calcd for $C_{26}H_{19}ClN_5O_2Ru^+$: *m*/*z* = 570.03); elemental analysis calcd (%) for $C_{26}H_{19}Cl_2N_5O_2Ru \cdot 3H_2O$: C 47.35, H 3.82, N 10.62; found: C 47.68, H 3.75, N 10.79.

[Ru(tpy)(bpy-COOH)Cl]Cl (9a). Yield: 41%; ^1H NMR (400 MHz, [D_6]DMSO): δ = 10.27 (d, ^3J(H,H) = 6.0 Hz, 1H; H_A), 9.28 (s, 1H; H_D), 9.0 (s, 1H; H_E), 8.86 (d, ^3J(H,H) = 8.0 Hz, 2H; H_e), 8.72 (d, ^3J(H,H) = 8.0 Hz, 2H; H_d), 8.45 (dd, ^3J(H,H) = 5.6 Hz, ^4J(H,H) = 1.2 Hz, 1H; H_B), 8.29 (t, ^3J(H,H) = 8.4 Hz, 1H; H_f), 8.01 (t, ^3J(H,H) = 7.6 Hz, 2H; H_c), 7.62 (m, 3H; $H_{a,G}$), 7.45 (ddd, ^3J(H,H) = 6.0 Hz, ^4J(H,H) = 1.2 Hz, 2H; H_H), 7.35 (t, ^3J(H,H) = 6.8 Hz, 2H; H_b). λ_{max} (MeOH) (ε (M^{-1} cm^{-1}): 513 nm (14.3 × 10^3). ESI-MS: *m*/*z*: 614 [(M−Cl)$^+$] (anal. calcd for $C_{27}H_{19}ClN_5O_4Ru^+$: *m*/*z* = 614.02); elemental analysis calcd (%) for $C_{27}H_{19}Cl_2N_5O_4Ru \cdot 4H_2O$: C 44.95, H 3.77, N 9.71; found: C 45.39, H 3.94, N 9.91.

[Ru(tpy-COOH)(bpy-CO_2H)Cl]Cl (10a). Yield: 31%; ^1H NMR (400 MHz, [D_6]DMSO): δ = 10.01 (d, ^3J(H,H) = 5.6 Hz, 1H; H_A), 8.97 (s, 2H; H_e), 8.93 (s, 1H; H_D), 8.64 (s, 1H; H_E), 8.62 (s, 2H; H_d), 8.22 (dd, ^3J(H,H) = 5.6 Hz, ^4J(H,H) = 1.6 Hz, 1H; H_B), 7.92 (ddd, ^3J(H,H) = 7.6 Hz, ^4J(H,H) = 1.2 Hz, 2H; H_c), 7.59 (d, ^3J(H,H) = 4.8 Hz, 2H; H_a), 7.33 (ddd, ^3J(H,H) = 5.6 Hz, ^4J(H,H) = 1.2 Hz, 2H; H_b), 7.30 (dd, ^3J(H,H) = 6.0 Hz, ^4J(H,H) = 1.6 Hz, 1H; H_G), 7.21 (d, ^3J(H,H) = 5.6 Hz, 2H; H_H). λ_{max} (MeOH) (ε (M^{-1} cm^{-1}): 506 nm (14.3 × 10^3). ESI-MS: *m*/*z*: 658 [(M−Cl)$^+$] (anal. calcd for $C_{28}H_{19}ClN_5O_6Ru^+$: *m*/*z* = 658.00); elemental analysis calcd (%) for $C_{28}H_{19}Cl_2N_5O_6Ru \cdot 3H_2O$: C 44.99, H 3.37, N 9.37; found: C 45.21, H 3.54, N 9.41.

General Synthetic Procedure for [Ru(tpy-R^1)(bpy-R^2)(OH_2)]-(ClO_4)$_2$ (1b−10b). [Ru(tpy-R^1)(bpy-R^2)Cl]Cl (0.17 mmol) (**1a**−**10a**) was combined with $AgClO_4$ (0.34 mmol) and refluxed in 30 mL of H_2O for 3 h. The red/purple mixture was filtered through Celite. The volume of the filtrate was reduced followed by the addition of 5 mL of 1 M $HClO_4$ to precipitate the product. The purple solid was then washed with 5 mL of 1 M $HClO_4$ and left to air-dry. Yields and characterization data are specified below.

[Ru(tpy)(bpy)(OH$_2$)](ClO$_4$)$_2$ (1b). Yield: 76%; ^{1}H NMR (400 MHz, [D$_6$]DMSO): δ = 9.50 (d, ^3J(H,H) = 5.0 Hz, 1H; H_A), 8.95 (d, ^3J(H,H) = 8.2 Hz, 1H; H_D), 8.88 (d, ^3J(H,H) = 8.2 Hz, 2H; H_e), 8.74 (d, ^3J(H,H) = 7.9 Hz, 2H; H_d), 8.64 (d, ^3J(H,H) = 7.9 Hz, 1H; H_E), 8.43 (ddd, ^3J(H,H) = 7.9, 7.8 Hz, ^4J(H,H) = 1.2 Hz, 1H; H_C), 8.33 (t, ^3J(H,H) = 8.1 Hz, 1H; H_f), 8.15 (ddd, ^3J(H,H) = 7.0, 5.7 Hz, ^4J(H,H) = 1.0 Hz, 1H; H_B), 8.07 (ddd, ^3J(H,H) = 7.9, 7.8 Hz, ^4J(H,H) = 1.2 Hz, 2H; H_c), 7.79 (ddd, ^3J(H,H) = 8.0, 7.9 Hz, ^4J(H,H) = 1.3 Hz, 1H; H_F), 7.69 (d, ^3J(H,H) = 5.4 Hz, 2H; H_a), 7.45 (ddd, ^3J(H,H) = 7.5, 5.5 Hz, ^4J(H,H) = 1.2 Hz, 2H; H_b), 7.32 (d, ^3J(H,H) = 5.6 Hz, 1H; H_H), 7.09 (ddd, ^3J(H,H) = 8.0, 7.9 Hz, ^4J(H,H) = 1.3 Hz, 1H; H_G), 5.89 (s, 2H; Ru−OH_2). λ_{max} (H$_2$O) (ε (M^{-1} cm^{-1}): 476 nm (8.4 × 10^3). ESI-MS: *m*/*z*: 590 [(M−H$_2$O−ClO$_4$)$^+$] (anal. calcd for $C_{25}H_{19}ClN_5O_4Ru^+$: *m*/*z* = 590.02); elemental analysis calcd (%) for $C_{25}H_{21}Cl_2N_5O_9Ru$: C 42.44, H 2.99, N 9.90; found: C 42.24, H 3.03, N 9.86.

[Ru(tpy-OMe)(bpy)(OH$_2$)](ClO$_4$)$_2$ (2b). Yield: 52%; ^{1}H NMR (400 MHz, D$_2$O): δ = 9.55 (d, ^3J(H,H) = 5.6 Hz, 1H; H_A), 8.68 (d, ^3J(H,H) = 8.0 Hz, 1H; H_D), 8.46 (d, ^3J(H,H) = 8.4 Hz, 2H; H_d), 8.36−8.31 (m, 2H; $H_{E,C}$), 8.26 (s, 2H; H_e), 8.03−7.97 (m, 3H; $H_{B,c}$), 7.84 (d, ^3J(H,H) = 4.8 Hz, 2H; H_a), 7.70 (t, ^3J(H,H) = 7.6 Hz, 1H; H_F), 7.44 (d, ^3J(H,H) = 5.6 Hz, 1H; H_H), 7.34 (t, ^3J(H,H) = 6.4 Hz, 2H; H_b), 6.99 (t, ^3J(H,H) = 6.4 Hz, 1H; H_G), 4.28 (s, 3H; OMe). λ_{max} (H$_2$O) (ε (M^{-1} cm^{-1}): 479 nm (9.7 × 10^3). ESI-MS: *m*/*z*: 650 [(M−H$_2$O−ClO$_4$)$^+$] (anal. calcd for $C_{27}H_{23}ClN_5O_6Ru^+$: *m*/*z* = 650.04); elemental analysis calcd (%) for $C_{26}H_{23}Cl_2N_5O_{10}Ru\cdot H_2O$: C 41.34, H 3.34, N 9.27; found: C 41.22, H 3.53, N 9.14.

[Ru(tpy)(bpy-OMe)(OH$_2$)](ClO$_4$)$_2$ (3b). Yield: 64%; ^{1}H NMR (400 MHz, [D$_6$]DMSO): δ = 9.25 (d, ^3J(H,H) = 6.5 Hz, 1H; H_A), 8.84 (d, ^3J(H,H) = 8.1 Hz, 2H; H_e), 8.71 (d, ^3J(H,H) = 8.1 Hz, 2H; H_d), 8.60 (d, ^4J(H,H) = 2.6 Hz, 1H; H_D), 8.29 (d, ^4J(H,H) = 2.6 Hz, 1H; H_E), 8.26 (t, ^3J(H,H) = 8.1 Hz, 1H; H_f), 8.05 (ddd, ^3J(H,H) = 6.9, 6.8 Hz, ^4J(H,H) = 1.4 Hz, 2H; H_c), 7.82 (dd, 1H, ^3J(H,H) = 6.5 Hz, ^4J(H,H) = 2.6 Hz; H_B), 7.79 (d, ^3J(H,H) = 4.8 Hz, 2H; H_a), 7.47 (ddd, ^3J(H,H) = 6.8, 6.5 Hz, ^4J(H,H) = 1.1 Hz, 2H; H_b), 6.94 (d, ^3J(H,H) = 6.7 Hz, 1H; H_H), 6.69 (d, ^3J(H,H) = 6.7, ^4J(H,H) = 2.6 Hz, 1H; H_G), 5.65 (s, 2H; Ru−OH_2), 4.20 (s, 3H; *OMe*), 3.83 (s, 3H; *OMe*). λ_{max} (H$_2$O) (ε (M^{-1} cm^{-1}): 483 nm (9.9 × 10^3). ESI-MS: *m*/*z*: 650 [(M−H$_2$O−ClO$_4$)$^+$] (anal. calcd for $C_{27}H_{23}ClN_5O_6Ru^+$: *m*/*z* = 650.04); elemental analysis calcd (%) for $C_{27}H_{25}Cl_2N_5O_{11}Ru\cdot H_2O$: C 41.28, H 3.46, N 8.92; found: C 41.24, H 3.39, N 8.80.

[Ru(tpy-OMe)(bpy-OMe)(OH$_2$)](ClO$_4$)$_2$ (4b). Yield: 42%; ^{1}H NMR (400 MHz, D$_2$O): δ = 9.30 (d, ^3J(H,H) = 6.4 Hz, 1H; H_A), 8.44 (d, ^3J(H,H) = 8.0 Hz, 2H; H_d), 8.24 (s, 2H; H_e), 8.19 (s, 1H; H_D), 7.98 (t, ^3J(H,H) = 8.0 Hz, 2H; H_c), 7.91 (d, ^3J(H,H) = 5.6 Hz, 2H; H_a), 7.87 (d, ^4J(H,H) = 2.4 Hz, 1H; H_E), 7.65 (dd, ^3J(H,H) = 6.4 Hz, ^4J(H,H) = 2.4 Hz, 1H; H_B), 7.37 (t, ^3J(H,H) = 6.4 Hz, 2H; H_b), 7.13 (d, ^3J(H,H) = 6.4 Hz, 1H; H_H), 6.60 (dd, ^3J(H,H) = 6.4 Hz, ^4J(H,H) = 1.2 Hz, 1H; H_G), 4.27 (s, 3H; OMe), 4.23 (s, 3H; OMe), 3.85 (s, 3H; OMe). λ_{max} (H$_2$O) (ε (M^{-1} cm^{-1}): 487 nm (10.2 × 10^3). ESI-MS: *m*/*z*: 680 [(M−H$_2$O−ClO$_4$)$^+$] (anal. calcd for $C_{28}H_{25}ClN_5O_7Ru^+$: *m*/*z* = 680.05); elemental analysis calcd (%) for $C_{28}H_{27}Cl_2N_5O_{12}Ru$: C, 42.17; H, 3.41; N, 8.78. Found: C, 41.97; H, 3.73; N, 8.67.

[Ru(tpy-Cl)(bpy)(OH$_2$)](ClO$_4$)$_2$ (5b). Yield = 67%; ^{1}H NMR (400 MHz, [D$_6$]DMSO): δ = 9.48 (d, ^3J(H,H) = 4.8 Hz, 1H; H_A), 9.15 (s, 2H; H_e), 8.96 (d, ^3J(H,H) = 8.0 Hz, 1H; H_D), 8.81 (d, ^3J(H,H) = 8.0 Hz, 2H; H_d), 8.64 (d, ^3J(H,H) = 8.0 Hz, 1H; H_E), 8.44 (ddd, ^3J(H,H) = 8.0 Hz, ^4J(H,H) = 1.2 Hz, 1H; H_C), 8.15 (ddd, ^3J(H,H) = 5.6 Hz, ^4J(H,H) = 1.2 Hz, 1H; H_B), 8.10 (ddd, ^3J(H,H) = 8.0 Hz, ^4J(H,H) = 1.2 Hz, 2H; H_c), 7.80 (ddd, ^3J(H,H) = 7.6 Hz, ^4J(H,H) = 1.2 Hz, 1H; H_F), 7.71 (d, ^3J(H,H) = 5.2 Hz, 1H; H_a), 7.48 (m, 3H; $H_{b,H}$), 7.07 (ddd, ^3J(H,H) = 6.0 Hz, ^4J(H,H) = 1.2 Hz, 1H; H_G), 5.88 (s, 2H; H$_2$O). λ_{max} (H$_2$O) (ε (M^{-1} cm^{-1}): 478 nm (10.8 × 10^3). ESI-MS: *m*/*z*: 624 [(M−H$_2$O−ClO$_4$)$^+$] (anal. calcd for $C_{25}H_{18}Cl_2N_5O_4Ru^+$: *m*/*z* = 623.98); elemental analysis calcd (%) for $C_{25}H_{20}Cl_3N_5O_9Ru\cdot H_2O$: C 39.51, H 2.92, N 9.22; found: C 39.30, H 3.00, N 9.18.

[Ru(tpy)(bpy-Cl)(OH$_2$)](ClO$_4$)$_2$ (6b). Yield: 72%; ^{1}H NMR (400 MHz, [D$_6$]DMSO): δ: 9.40 (d, ^3J(H,H) = 4.0 Hz, 1H; H_A), 9.28 (d, ^4J(H,H) = 2.0 Hz, 1H; H_D), 8.98 (d, ^4J(H,H) = 2.4 Hz, 1H; H_E), 8.87 (d, ^3J(H,H) = 8.0 Hz, 2H; H_e), 8.73 (d, ^3J(H,H) = 8.0 Hz, 2H; H_d), 8.34 (m, 2H; $H_{B,f}$), 8.08 (ddd, ^3J(H,H) = 7.6 Hz, ^4J(H,H) = 1.2 Hz, 2H; H_c), 7.79 (d, ^3J(H,H) = 4.8 Hz, 2H; H_a), 7.45 (ddd, ^3J(H,H) = 6.0 Hz, ^4J(H,H) = 1.2 Hz, 2H; H_b), 7.32 (d, ^3J(H,H) = 6.4 Hz, 1H; H_G), 7.22 (ddd, ^3J(H,H) = 6.0 Hz, ^4J(H,H) = 2.0 Hz, 1H; H_H), 5.95 (s, 2H; H$_2$O). λ_{max} (H$_2$O) (ε (M^{-1} cm^{-1}): 490 nm (11.9 × 10^3). ESI-MS: *m*/*z*: 660 [(M−H$_2$O−ClO$_4$)$^+$] (anal. calcd for $C_{25}H_{17}Cl_3N_5O_4Ru^+$: *m*/*z* = 659.94); elemental analysis calcd (%) for $C_{25}H_{19}Cl_4N_5O_9Ru\cdot H_2O$: C 37.80, H 2.66, N 8.82; found: C 38.23, H 2.39, N 8.83.

[Ru(tpy-Cl)(bpy-Cl)(OH$_2$)](ClO$_4$)$_2$ (7b). Yield: 26%; poor yield is due to low solubility of [Ru(tpy-Cl)(bpy-Cl)Cl]Cl in water. ^{1}H NMR (400 MHz, [D$_6$]DMSO): δ = 9.37 (d, ^3J(H,H) = 6.4 Hz, 1H; H_A), 9.28 (s, 1H; H_D), 9.14 (s, 2H; H_e), 8.98 (s, 1H; H_E), 8.79 (d, ^3J(H,H) = 8.0 Hz, 2H; H_d), 8.32 (d, ^3J(H,H) = 4.8 Hz, 1H; H_B), 8.11 (t, ^3J(H,H) = 7.6 Hz, 2H; H_c), 7.81 (d, ^3J(H,H) = 4.8 Hz, 2H; H_a), 7.47 (m, 3H; $H_{G,b}$), 7.19 (d, ^3J(H,H) = 4.8 Hz, 1H; H_H), 5.94 (s, 2H; H$_2$O). λ_{max} (H$_2$O) (ε (M^{-1} cm^{-1}): 493 nm (13.0 × 10^3). ESI-MS: *m*/*z*: 694 [(M−H$_2$O−ClO$_4$)$^+$] (anal. calcd for $C_{25}H_{16}Cl_4N_5O_4Ru^+$: *m*/*z* = 693.90); elemental analysis calcd (%) for $C_{25}H_{18}Cl_5N_5O_9Ru$: C 37.03, H 2.24, N 8.64; found: C 37.43, H 2.30, N 8.70.

[Ru(tpy-COOH)(bpy)(OH$_2$)](ClO$_4$)$_2$ (8b). Yield: 75%; ^{1}H NMR (400 MHz, D$_2$O): δ = 9.58 (d, ^3J(H,H) = 5.2 Hz, 1H; H_A), 9.05 (s, 2H; H_e), 8.73 (d, ^3J(H,H) = 8.0 Hz, 1H; H_D), 8.58 (d, ^3J(H,H) = 8.0 Hz, 2H; H_d), 8.38 (m, 2H; $H_{E,C}$), 8.09 (t, ^3J(H,H) = 6.4 Hz, 1H; H_B), 8.04 (t, ^3J(H,H) = 7.6 Hz, 2H; H_c), 7.83 (d, ^3J(H,H) = 5.2 Hz, 2H; H_a), 7.72 (t, ^3J(H,H) = 7.2 Hz, 1H; H_F), 7.40 (t, ^3J(H,H) = 6.8 Hz, 2H; H_b), 7.28 (d, ^3J(H,H) = 5.6 Hz, 1H; H_H), 6.95 (t, ^3J(H,H) = 6.8 Hz, 1H; H_G). λ_{max} (H$_2$O) (ε (M^{-1} cm^{-1}): 484 nm (9.6 × 10^3). ESI-MS: *m*/*z*: 634 [(M−H$_2$O−ClO$_4$)$^+$] (anal. calcd for $C_{26}H_{19}ClN_5O_6Ru^+$: *m*/*z* = 634.01); elemental analysis calcd (%) for $C_{26}H_{21}Cl_2N_5O_{11}Ru\cdot 2H_2O$: C 39.66, H 3.20, N 8.89; found: C 39.29, H 3.05, N 8.83.

[Ru(tpy)(bpy-COOH)(OH$_2$)](ClO$_4$)$_2$ (9b). Yield: 90%; ^{1}H NMR (400 MHz, D$_2$O): δ = 9.67 (d, ^3J(H,H) = 6.0 Hz, 1H; H_A), 9.16 (d, ^4J(H,H) = 1.2 Hz, 1H; H_D), 8.81 (d, ^4J(H,H) = 1.6 Hz, 1H; H_E), 8.55 (d, ^3J(H,H) = 8.0 Hz, 2H; H_e), 8.41 (m, 3H; $H_{d,B}$), 8.22 (t, ^3J(H,H) = 8.0 Hz, 1H; H_f), 7.92 (ddd, ^3J(H,H) = 8.0 Hz, ^4J(H,H) = 1.6 Hz, 2H; H_c), 7.65 (d, ^3J(H,H) = 5.6 Hz, 2H; H_a), 7.54 (d, ^3J(H,H) = 8.0 Hz, ^4J(H,H) = 1.2 Hz, 2H; H_G), 7.34 (dd, ^3J(H,H) = 6.0 Hz, ^4J(H,H) = 1.6 Hz, 1H; H_H), 7.26 (ddd, ^3J(H,H) = 5.6 Hz, ^4J(H,H) = 1.2 Hz, 2H; H_b). λ_{max} (H$_2$O) (ε (M^{-1} cm^{-1}): 488 nm (12.7 × 10^3). ESI-MS: *m*/*z*: 678 [(M−H$_2$O−ClO$_4$)$^+$] (anal. calcd for $C_{27}H_{19}ClN_5O_8Ru^+$: *m*/*z* = 678.00); elemental analysis calcd (%) $C_{27}H_{21}Cl_2N_5O_{13}Ru\cdot 5H_2O$: C 36.62, H 3.53, N 7.91; found: C 36.28, H 3.12, N 7.84.

[Ru(tpy-CO$_2$H)(bpy-COOH)(OH$_2$)](ClO$_4$)$_2$ (10b). Yield: 77%; ^{1}H NMR (400 MHz, D$_2$O): δ = 9.58 (d, ^3J(H,H) = 6.0 Hz, 1H; H_A), 8.90 (d, ^4J(H,H) = 1.2 Hz, 1H; H_D), 8.75 (s, 2H; H_e), 8.54 (s, ^4J(H,H) = 1.2 Hz, 1H; H_E), 8.36 (d, ^3J(H,H) = 8.0 Hz, 2H; H_d), 8.21 (dd, ^3J(H,H) = 6.0 Hz, ^4J(H,H) = 2.0 Hz, 1H; H_B), 7.80 (ddd, ^3J(H,H) = 7.6 Hz, ^4J(H,H) = 1.6 Hz, 2H; H_c), 7.54 (d, ^3J(H,H) = 4.8 Hz, 2H; H_a), 7.16 (m, 3H; $H_{G,b}$), 7.02 (dd, ^3J(H,H) = 6.0 Hz, ^4J(H,H) = 2.0 Hz, 1H; H_G). λ_{max} (H$_2$O) (ε (M^{-1} cm^{-1}): 494 nm (11.9 × 10^3). ESI-MS: *m*/*z*: 722 [(M−H$_2$O−ClO$_4$)$^+$] (anal. calcd for $C_{28}H_{19}ClN_5O_{10}Ru^+$: *m*/*z* = 721.99); elemental analysis calcd (%) for $C_{28}H_{21}Cl_2N_5O_{15}Ru\cdot 4H_2O$: C 36.89, H 3.21, N 7.68; found: C 36.59, H 3.33, N 7.93.

Physical Methods. Electrochemical measurements were performed under anaerobic conditions, and recorded with a Princeton Applied Research VersaStat 3 potentiostat using dry solvents, a Pt or glassy carbon working electrode (diameter = 3 mm), a [Ag]/[AgCl] reference electrode, and 0.1 M HNO_3

supporting electrolyte unless otherwise specified. Potentials reported herein are referenced to a normal hydrogen electrode (NHE). Routine ^{1}H NMR spectra were recorded at 400 MHz on a Bruker Avance 400 instrument at ambient temperature. Elemental analysis and electrospray ionization (ESI) mass spectrometry (MS) data were collected at the University of Calgary Instrumentation Facility. Electronic spectroscopy data were collected using a Cary 5000 UV−vis spectrophotometer (Varian). Density functional theory (DFT) calculations were carried out using B3LYP (Becke's three-parameter exchange functional (B3) and the Lee−Yang−Parr correlation functional (LYP)) and the LanL2DZ basis set.[26,27] All geometries were fully optimized in the ground states (closed-shell singlet, S_o). All calculations were carried out with the Gaussian 03W software package.[28] Dioxygen evolution data was recorded using a custom-built apparatus consisting of a 10-mL round-bottom flask equipped with a septum and a threaded side arm for insertion of the probe; total working volume is 16.8 mL. The flask was charged with a solution of $(NH_4)_2[Ce(NO_3)_6]$ (0.33 M) in 1 M $HClO_4$ (3.0 mL), and the headspace was purged with $N_{2(g)}$. A deaerated solution containing 5.0×10^{-8}−5.0×10^{-7} mol of the catalyst was then injected through a rubber septum, and stirred at ambient temperatures (24 ± 2 °C) for the duration of the experiment. The rate of oxygen evolution is linearly proportional to the catalyst concentration to indicate first-order behavior. Dioxygen evolution was monitored every 10 s with an optical probe (Ocean Optics FOXY-OR125-AFMG) and a multifrequency phase fluorimeter (Ocean Optics MFPF-100). Raw data from the sensor was collected by the TauTheta Host Program and then converted into the appropriate calibrated O_2 sensor readings in "%O_2" by the OOISensors application.

Results and Discussion

Catalytic water oxidation studies of **1a** and **1b**−**10b** were carried out using previously established protocols as a guide: Ce(IV) (in excess) was utilized as the sacrificial oxidant in 1 M $HClO_4$; O_2 evolution was quantified with an optical probe in the headspace of the closed reaction vessel.[29,30] Because a direct comparison of catalytic behavior for documented water oxidation catalysts is rendered difficult by the diverse set of reaction conditions used by different research groups (Supporting Information, Table S1), we also provide the performance of a well-defined catalyst recently reported by Meyer et al.,[14] $[Ru(tpy)(bpm)(OH_2)]^{2+}$ (**11**; bpm = 2,2′-bipyrimidine, Figure 1), recorded under our reaction conditions to serve as a comparison. We note that the oxidation of water in the presence of Ce(IV) is thermodynamically favorable (eq 1),[31] but the amount of oxygen formed on the time scale of our experiments is negligible; the presence of a Ru catalyst results in a significant increase in the rate of dioxygen evolution. The possibility that $RuO_2 \cdot xH_2O$, a potential decomposition product, is a significant source of oxygen production is ruled out on the basis that: (i) commercial RuO_2 and several less-stable Ru complexes (listed in Supporting Information, Figure S1) did not produce significant quantities of oxygen (i.e., amount of O_2 generated is equivalent to TON = 5); (ii) the catalyst can be recovered when 30 equiv of Ce(IV) is added to **1b**;[15] and (iii) RuO_2 at the Ce/Ru molar ratio used in our experiments oxidizes to form catalytically inactive RuO_4.[32,33] All of the compounds listed in Figure 1 were found to be competent catalysts under said conditions; however, the aqua-ligated species **1b**−**10b** exhibited a shorter induction period and a higher initial rate relative to the Cl^--ligated derivatives **1a**−**10a**. The initial phase of our experiments were designed to unravel this disparate behavior, and to identify sources of catalyst deactivation/decomposition. Studies were then carried out to delineate how catalyst activity and stability is affected by the identity of the terminal substituents. Results from this series of experiments are outlined accordingly below.

$$4Ce^{IV} + 2H_2O \underset{1\ M\ HClO_4}{\rightleftharpoons} O_2 + 4H^+ + 4Ce^{III} \qquad E^\circ = +0.47\ V \qquad (1)$$

Identity of Active Form of Catalyst. The notion that mononuclear polypyridyl Ru complexes are capable of catalyzing the oxidation of water has only recently gained traction.[13−15] Given that dioxygen formation was observed using compounds structurally related to **1a**, it was proposed that these complexes undergo an expansion of the primary coordination sphere to retain the Ru−Cl bond within the catalytic cycle.[13] A series of experiments by Sakai et al.,[15] however, have suggested that the catalytically active form of the catalyst is the $Ru-OH_2$ species, **1b**. The dioxygen evolution data recorded on the halide- and aqua-ligated compounds suggests that the Ru−Cl complexes **1a**−**10a** serve as "pre-catalysts" to their respective analogues **1b**−**10b** (Supporting Information, Figure S2).

Using proton H_A (or H_A·) as a spectroscopic handle, we used ^{1}H NMR spectroscopy to gain a better understanding of the behavior of these complexes in solution (Figure 3). The spectrum of **1a**, for example, shows that the Ru−Cl bond is retained in [D$_6$]DMSO (Figure 3a). When this complex is dissolved in D_2O, however, the spectral profile of $[Ru(tpy)(bpy)(OD_2)]^{2+}$ emerges (Figure 3b) producing significant quantities of the aqua-ligated species within 3 h (Figure 3c). Taking into consideration that C_s symmetry is preserved, **1a** is converted to **1b** in aqueous media. This process is accelerated in acidic media: the pseudo-first order rate constants of Cl^- displacement by D_2O for **1a** are 8.0×10^{-5} and 9.7×10^{-5} s^{-1} in D_2O and 0.1 M H_2SO_4, respectively (Figures 3 and S3 in the Supporting Information). Halide substitution by H_2O in acidic media was also verified by UV−vis experiments (Supporting Information, Figure S4). Similar behavior was observed for **2a**−**10a**, but the rate of Cl^- exchange by D_2O is faster when ligands bearing electron-donating groups (EDGs) are used; that is, the relative rate of Cl^- displacement by solvent follows **3a** > **1a** > **6a** (note that the Cl^- ligand of **1a** is not displaced by [D$_6$]DMSO or CD_3CN over a 1 week period; Figure 3a). The increased lability of the halide ligand is ascribed to increased electronic repulsion between the filled Ru and Cl^- π-orbitals.

(26) Frisch, M. J.; Pople, J. A.; Binkley, J. S. *J. Chem. Phys.* **1984**, *80*, 3265–9.
(27) Gill, P. M. W.; Johnson, B. G.; Pople, J. A.; Frisch, M. J. *Chem. Phys. Lett.* **1992**, *197*, 499–505.
(28) Frisch, M. J. et al. *Gaussian 03*, Revision c.02; Gaussian Inc.: Wallingford, CT, 2004.
(29) Deng, Z. P.; Tseng, H. W.; Zong, R. F.; Wang, D.; Thummel, R. *Inorg. Chem.* **2008**, *47*, 1835–1848.
(30) Kanan, M. W.; Surendranath, Y.; Nocera, D. G. *Chem. Soc. Rev.* **2009**, *38*, 109–114.
(31) Mills, A. *Chem. Soc. Rev.* **1989**, *18*, 285–316.
(32) Kiwi, J.; Gratzel, M.; Blondeel, G. *J. Chem. Soc., Dalton Trans.* **1983**, 2215–2216.
(33) Mills, A. *J. Chem. Soc., Dalton Trans.* **1982**, 1213–1216.

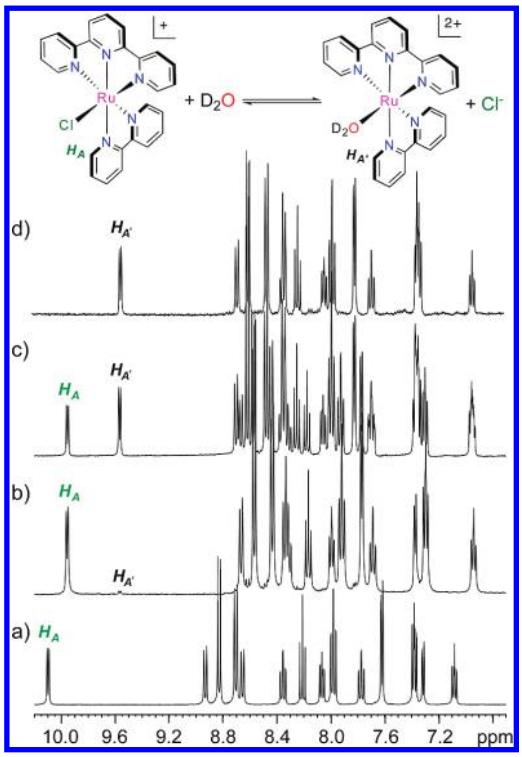

Figure 3. ^{1}H NMR spectra highlighting the conversion of **1a** to **1b** in aqueous media: (a) **1a** in [D_6]DMSO; (b) **1a** in D_2O after 5 min; (c) **1a** in D_2O after 3 h (relative concentrations of **1a** and **1b** are 45% and 55%, respectively); (d) **1b** in D_2O.

These observations collectively indicate that water oxidation by catalysts related to **1a** are more likely to adhere to a mechanism proposed by Meyer et al.,[14] and decreases the likelihood that a 7-coordinate intermediate occurs to retain the Ru−Cl bond[34] (we note that the expansion of the first coordination sphere may still occur in systems with strained ligand environments[13,35]). Our assessment is substantiated by the following observations: (i) there is a longer observed induction period for **1a** relative to **1b** in the dioxygen evolution experiments (i.e., **1b** exhibits higher catalytic activity than **1a**; see Supporting Information, Figure S2); (ii) the catalytic activity of **1b** is suppressed by competing solvents (e.g., MeCN) and/or anions (e.g., Cl^-[15]); (iii) the Ru(IV) (and Ru(V)) oxidation level is not accessible within the solvent window for **1a** because of a lack of charge stabilization by PCET processes (vide infra); and (iv) significant quantities of **1b** are observed by UV−vis and NMR experiments when **1a** is dissolved in (acidic) aqueous media.

Catalyst Deactivation. With the recognition that the aqua-ligated compounds **1b**−**10b** exhibit higher catalytic activity, experiments were carried out to examine the fate of **1b** to elucidate possible deactivation pathways. For instance, the workup of a reaction involving the addition of 1000 equiv of Ce(IV) to **1b** in acidic media revealed that a significant quantity of 2,2′-bipyridine *N,N*′-dioxide (bpydo) was produced (Supporting Information, Figure S5). This same species was observed by electrospray-ionization mass spectrometry (ESI-MS) in independent

(34) Tseng, H. W.; Zong, R.; Muckerman, J. T.; Thummel, R. *Inorg. Chem.* **2008**, *47*, 11763–11773.
(35) Duan, L. L.; Fischer, A.; Xu, Y. H.; Sun, L. C. *J. Am. Chem. Soc.* **2009**, *131*, 10397–10399.

Table 1. Bond Lengths (in Å) for **1b** and Potential Higher-Valent Ru Catalytic Intermediates Determined by DFT[a]

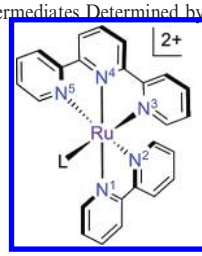

[Ru(tpy)(bpy)(L)]$^{2+}$	Ru-N^1	Ru-N^2
[Ru(tpy)(bpy)(OH$_2$)]$^{2+}$	2.101	2.056
[Ru(tpy)(bpy)(OH)]$^{2+}$	2.101	2.125
[Ru(tpy)(bpy)(O)]$^{2+}$	2.112	2.203

[a] A numbering scheme for the N atoms is provided.

experiments. On this basis, the dissociation of bpy likely represents a deactivation pathway. Note that bpydo is not generated when bpy is stirred in a 1 M $HClO_4$ solution containing 1000 equiv of Ce(IV). In light of these results, we contend that the generation of this organic byproduct under acidic, oxidizing reaction conditions should be taken into consideration for related ligands in other systems.

There was no evidence to support the dissociation of tpy from the metal site in said decomposition experiments. While this observation may be attributed solely to the chelate effect, we explored this point in further detail by examining the relative metal−ligand bond distances of geometry-optimized structures calculated by DFT (Table 1 and Supporting Information, Table S2). An examination of the bond distances for a series of likely intermediates derived from **1b** within a plausible catalytic cycle (e.g., cycle proposed by Meyer et al.[18,36]) reveals no appreciable change in the Ru−N_{tpy} bond distances (Supporting Information, Table S3). While the same holds true for the Ru−N^1 bond *cis* to L, the Ru−N^2 bond *trans* to the Ru−O bond(s) increases significantly at higher oxidation levels. This feature presumably increases the lability of the Ru−N_{bpy} bond to provide a deactivation pathway that ultimately leads to the loss of bpy.

Correlation of Catalytic Performance to Electronic Parameters. Having established the catalytic behavior of **1b**, we modified the polypyridyl scaffold of the complex with various EDGs and electron-withdrawing groups (EWGs) to furnish **2b**−**10b** (Figure 1). These compounds present the opportunity to systematically analyze how the π-accepting nature of the polypyridyl ligands affect catalyst performance under conditions relevant to water oxidation (a full complement of characterization data is provided in Table 2). Electrochemical data recorded in aqueous media for **1b**−**10b** and **11** show that higher oxidation levels are accessible as a consequence of PCET steps stabilizing the charge of the complex. Cyclic voltammograms of the aqua-ligated complexes are generally characterized by two reversible 1e$^-$ oxidation processes accompanied with H^+ loss to produce [Ru(tpy-R^1)(bpy-R^2)(OH)]$^{2+}$ and [Ru(tpy-R^1)(bpy-R^2)(O)]$^{2+}$ in succession. The 1e$^-$ oxidation of the respective Ru(IV)-oxo species are observed along with a catalytic wave corresponding to water oxidation. The trends in the electrochemical data for the series are consistent with the nature (i.e., π-donor: −OMe; π-acceptor: −COOH; π-donor/σ-acceptor: −Cl), number, and position of the substituents about the polypyridyl framework. A feature that is

(36) Chen, Z.; Concepcion, J. J.; Jurss, J. W.; Meyer, T. J. *J. Am. Chem. Soc.* **2009**, *131*, 15580–15581.

Table 2. Summary of Electrochemical Data and Catalytic Parameters for **1a**, **1b**−**10b**, and **11**

		$E_{1/2}$(V vs NHE)[a]				
class	compound	Ru(III)/(II)	Ru(IV)/(III)	Ru(V)/(IV)[b]	k_{obs} ($\times 10^{-4}$ s^{-1})[c]	TON[d]
parent	**1a**	1.05[e]			3.7	290
	1b	1.04	1.15	1.73	5.1	320
−OMe	**2b**	0.99	1.19	1.69	5.2	200
	3b	0.91	1.18	1.63	11	100
	4b	0.87	1.11	1.65	12	60
−Cl	**5b**	1.07	1.13	1.74	5.4	270
	6b	1.11	1.16	1.71	2.6	480
	7b	1.16	1.21	1.74	2.8	400
−COOH	**8b**	1.11	–[f]	1.80	6.8	210
	9b	1.16	–[f]	1.80	2.0	460
	10b	1.20	–[f]	1.82	3.3	200
other	**11**[14]	1.17	< 1.17	1.70	6.0	50

[a] Samples (1 mM) dissolved in 0.1 M $HNO_{3(aq)}$ (pH = 1.07) were measured at 50 mV/s and referenced to a Ag/AgCl (3 M NaCl) electrode followed by conversion to NHE ($[Ag]^0$/[AgCl] vs NHE = 210 mV) unless otherwise indicated. Assignment of proton-coupled oxidation waves are indicated: Ru(II) = $[Ru(II)-OH_2]^{2+}$; Ru(III) = $[Ru(III)-OH]^{2+}$; Ru(IV) = $[Ru(IV)=O]^{2+}$; and Ru(V) = $[Ru(V)=O]^{3+}$. [b] Redox process can be difficult to identify within onset of catalytic oxidation of H_2O; $E_{p,a}$ indicated. [c] First-order rate constant (±10%) was extracted by an exponential fitting of O_2 evolution data as a function of time.[37] [d] TON = catalytic turnovers after 3 h; defined as *mol O_2/mol catalyst*. [e] Recorded in a 0.1 M NH_4BF_4 MeCN solution at 100 mV/s and referenced to a $[Fc]/[Fc]^+$ internal standard; reported vs NHE ($[Fc]/[Fc]^+$ vs NHE = 0.64 V). [f] Not observed under our conditions.

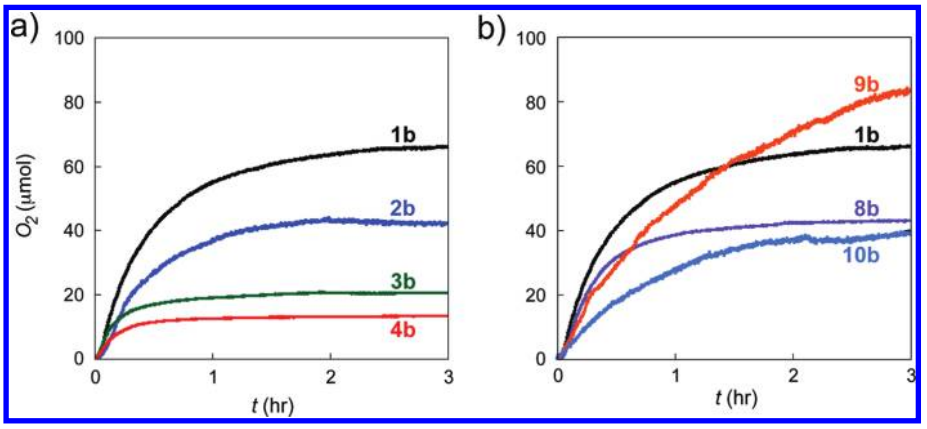

Figure 4. O_2 evolution data for the (a) −OMe and (b) −COOH series. The parent compound **1b** is provided as a benchmark in both plots.

of particular relevance to water oxidation is the observation that the Ru(V)/(IV) oxidation potential is lowest for the −OMe series **2b**−**4b** (∼+1.7 V), while the −COOH substituents lead to the highest oxidation potentials (∼+1.8 V). The Ru(IV)/(III) redox process for compounds bearing the −COOH substituents (i.e., **8b**−**10b**) could not be resolved. The observation that these two waves are resolved for the −Cl series, **5b**−**7b**, highlights how the π-donating/-withdrawing character of the terminal substituents stabilizes different redox levels. Note that a single wave at +1.17 V corresponding to a $2e^-/2H^+$ process occurs for **11** in 1M $HClO_{4(aq)}$, a consequence of the lower thermodynamic stability of the $[Ru^{III}-OH]^{2+}$ species relative to the $[Ru^{IV}=O]^{2+}$ species.[14]

Under our reaction conditions, the oxidation of water driven by a large excess of Ce(IV) (maximum attainable TON is ca. 1200) in the presence of **1b**−**10b** does not, in general, occur at a significant rate beyond a 3 h period (Figure 4); the diminished of catalytic activity can be attributed to catalyst deactivation or decomposition. Consequently, the catalytic turnover number (TON) at this stage of the reaction provides an indirect measure of catalyst stability. The relative TONs for the −OMe series reveal that the additional electron density on the metal reduces catalyst stability (e.g., **2b** > **3b** > **4b**; Figure 4a). The presence of EWGs on the bpy ligand enhances catalytic stability; however, EWGs situated on the tpy ligand compromises catalytic stability (Figure 4b). An explanation of this trend can be rationalized by the diminished π-backbonding to the bpy ligands caused by the EWG on the tpy ligand, and highlights how optimal catalyst stability is a fine balance between electron density at the metal and π-backbonding to the most labile ligand. Catalysts **5b**−**7b** follow the same trend as **8b**−**10b**, which is consistent with the electron-withdrawing character of the halide substituents (Supporting Information, Figure S6). The relative stabilities of these compounds are consistent with trends in bond lengths of the optimized geometries for **1b**−**10b** calculated using DFT. While these observations have not been explicitly addressed in the literature, our conclusions are corroborated by assessing the relative TONs reported for other mononuclear catalysts.[13]

The rates of dioxygen evolution were all found to exhibit pseudo-first-order behavior with respect to catalyst concentration for **1b**−**10b** and **11**; thus, the rate constant could be extracted by fitting the data to an exponential function (Supporting Information, Figure S8).[37] The catalytic data presented in Table 2 reveals that higher k_{obs}

(37) Xu, Y. H.; Akermark, T.; Gyollai, V.; Zou, D. P.; Eriksson, L.; Duan, L. L.; Zhang, R.; Akermark, B.; Sun, L. C. *Inorg. Chem.* **2009**, *48*, 2717–2719.

values are generally observed for complexes bearing electron-donating substituents (e.g., **2b**−**4b**). We attribute this trend to the accessibility of the $Ru^{V}=O$ level, or the release of dioxygen from a $Ru^{IV}(O_2)$ or $Ru^{V}(O_2)$ complex enhanced by the presence of π-donating groups in the mechanism put forth by Meyer et al.[14] The fact that the −OMe series, which exhibit a Ru(V)/Ru(IV) couple at about 0.15 V less than the −COOH series, produces the highest k_{obs} values supports the notion that accessibility of the Ru(V) level represents a possible rate-determining step within the catalytic cycle. Catalyst deactivation may suppress the observed k_{obs} values because the competing rates of catalytic activity and decomposition are difficult to delineate under these conditions; studies are currently underway to further understand these events.

Conclusion

The suite of compounds presented in this study provides the opportunity to directly assess how electronic factors affect catalytic rate and stability in the context of water oxidation. An important outcome of this study is a strong correlation between catalyst activity and stability to the position and identity of various EDGs/EWGs on the polypyridyl ligands. It is also recognized that the bidentate ligands for catalysts related to **1b** are labile under conditions relevant to water oxidation, and the appropriate installation of EWGs can suppress this decomposition pathway. The recognition that the Ru−Cl bond is not robust in conditions relevant to water oxidation is also important in developing plausible mechanisms for the water-splitting reactions. Collectively, these factors provide some important clarification of the catalytic behavior of **1b** (and related systems), and should be considered in the collective pursuit of stable water-splitting catalysts.

Acknowledgment. The authors are grateful to Dr. J. Scott McIndoe (University of Victoria) for experimental assistance. This work was financially supported by the Natural Science and Engineering Research Council of Canada, Canada Foundation for Innovation, Canada Research Chairs, and Alberta Ingenuity.

Supporting Information Available: A ^{1}H NMR and UV−vis spectroscopic analysis of equilibrium between **1a** and **1b**, a summary of the bond distances calculated by DFT, and dioxygen evolution data are provided as Supporting Information. This material is available free of charge via the Internet at http://pubs.acs.org.